

Understanding of the flow separation phenomenon in space launchers nozzles

S. PALERM¹, H. LAMBARE²,
CNES, Centre Spatial d'Evry, Rond-Point de l'Espace – 91023 Evry, France

and

P. REIJASSE³
ONERA, Centre de Chalais-Meudon, 8 rue des Vertugadins – 92190 Meudon, France

Abstract – The ATAC group was created in the late 1990s on CNES and ONERA's initiative, and in cooperation with French laboratories and industrials, to investigate aerodynamics issues for space launchers nozzles and blunt bodies. This paper presents a synthesis of the research work done in the frame of the ATAC program to better understand the flow separation phenomenon in over expanded nozzles.

1. INTRODUCTION

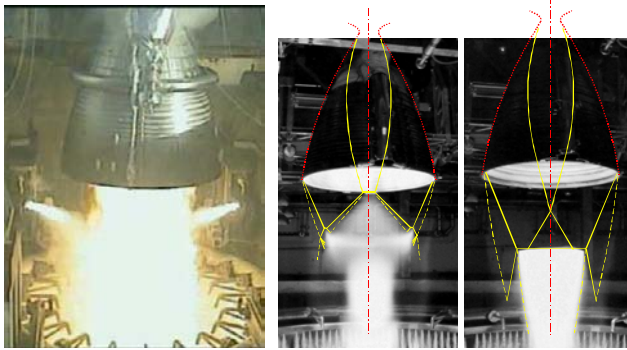


Figure 1 : Vulcain® engine at start up (SNECMA courtesy)

Heavy rockets use cryogenic second stages which engine is usually ignited at the launcher lift off. Therefore, the engine, optimized for the second phase of the launcher's flight at rather high altitudes, has to operate also in the first phase, at low altitudes. Thus, the nozzles of such engines are usually designed with a high sections ratio (ratio between the exit and throat sections), and, for the first seconds of the flight, the nozzle operates in over-expanded conditions where the atmospheric pressure is higher than the flow pressure at the nozzle exit.

Therefore, a flow separation occurs inside the nozzle, inducing high side loads and thermal loads. The side loads phenomenon results from both the three-dimensional and unsteady natures of this flow separation.

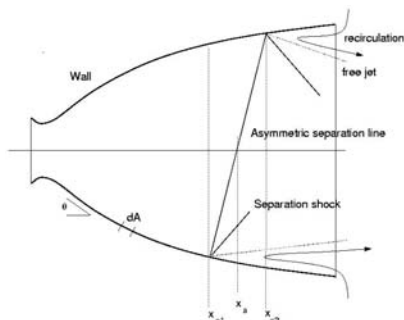


Figure 2 : three-dimensional shock structure in an overexpanded nozzle.

The most recent nozzle designs usually limit the separation in steady conditions to the very end of the nozzle. The surface then impacted by the separation is limited, and thus the momentum levels. However, the side loads remain an issue in transient conditions when the chamber pressure increases, for strong flow separations can not be avoided in such conditions, and usually induce the strongest momentum levels. This three-dimensional nature of the flow is associated with a large unsteadiness of the shock, which increases the difficulty to analyze this phenomenon properly since both the structure and the unsteadiness of the flow should be reproduced.

The understanding of the side loads phenomenon is at major stake in the ATAC program, and thus the subject of most of the experimental and numerical studies. Apart from the side loads effect, the three-dimensional nature of the flow induces a fluid/structure interaction which needs to be addressed to investigate some possible deformations of the structure due to the side loads, but also some modifications of the flow structure due to major movements of the nozzle. This has been done experimentally on flexible nozzles, but also numerically through the use and extension of the Pekkari model.

Lastly, if the thermal loads resulting from the flow separation are a slow phenomenon with few consequences during transient, their effects in steady conditions are strong, since, for this flow regime, the thermal transfers between flow and structure have time to occur, and alter significantly the material characteristics of the structure. The part of this investigation in the ATAC program, once limited by the test benches and the numerical tools capacities, is strongly increasing thanks to the improvements operated these last years on both experimental devices and numerical tools.

2. SIDE LOADS

As explained previously, the side loads are caused by the strong three-dimensional nature of the flow separation inside the nozzle. Before analyzing this three-dimensional effect the different flow structures occurring inside the nozzle have to be investigated.

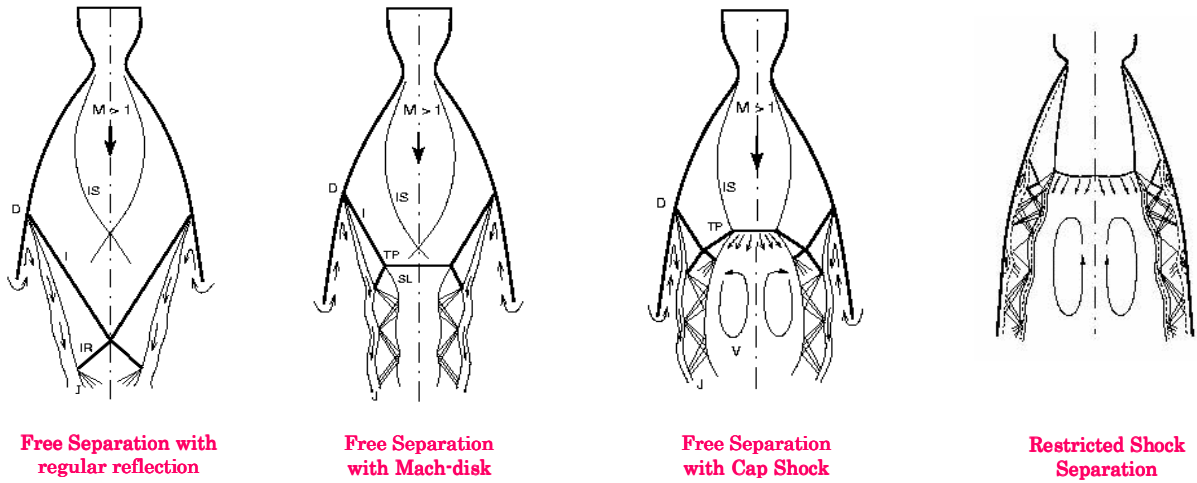


Figure 3 : visualisation of the different shock structures in an overexpanded nozzle.

In Truncated Ideal Contoured (TIC) nozzles, the flow separates from the wall without reattachment. This kind of flow is referenced to as Free Shock Separation(FSS), and shows two shock structures: a free separation with a regular reflection, and a free separation with a Mach disk reflection. This last structure is evidenced by a luminous disk shape on the exhaust plume (see Figure 1).

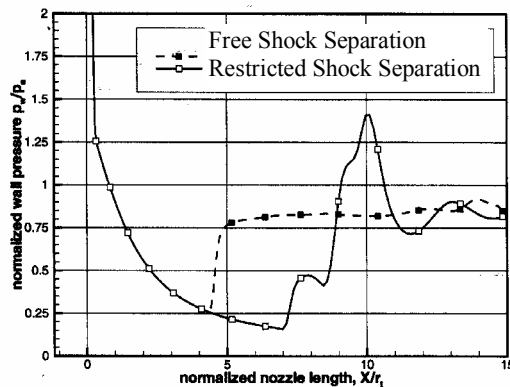


Figure 4 : wall pressure profile for FSS and RSS regimes

Cryogenic rocket engines mainly use Thrust Optimised Contoured (TOC) nozzles, which profile is very close to TIC ones, with identical sections ratios, but with a shorter length, for mass optimisation. This type of nozzles shows an internal shock due to the strong slope variation occurring at throat. The intersection of this internal shock with the Mach disk and the separated boundary layer creates a cap shock pattern [1] which may generate a Restricted Shock Separation, where the boundary layer reattaches after the separation, creating a recirculation bubble at the wall (Figure 3).

Therefore, four shock structures can be observed in TOC nozzles, depending on the pressure ratios and on the nozzle contour. From a general point of view, FSS and RSS regimes have a specific wall pressure profile (Figure 4), with a pressure rise behind the separation for both, and a peak at the reattachment position for the RSS regime.

As a first step, the understanding of the physical phenomena occurring in these flows has been carried out through the observation and the numerical simulation of a recirculation bubble on a simple cold gases planar facility at IUSTI. Then, the three-dimensional behaviour has been addressed with several experimental campaigns in cold gases reproducing subscale nozzle geometries and their dynamic behaviour, with a special care for the reproduction of the shock structures identified on full-scale hot gas nozzles. The latest experiments and numerical simulations deal with the transient aspects of a film cooling or of the chamber pressure ramping.

2.1 Shock wave/boundary layer interaction

The shock wave/boundary layer interaction is a physical phenomena which drives the overexpansion of the flow in the nozzle. This interaction is widely investigated at IUSTI [2] through an experimental set-up in a wind tunnel, which controls the incident shock position on the boundary layer (see Figure 5), for long duration runs. This set-up is a planar one which allows a direct visualisation of the phenomenon for optic measurement techniques, and easier correlations in transverse direction. An intense use of PIV measurements lead to the creation of a large database including informations on the speed fluctuations (Figure 6), which are very usefull, both for the physical understanding and the numerical tool validation.

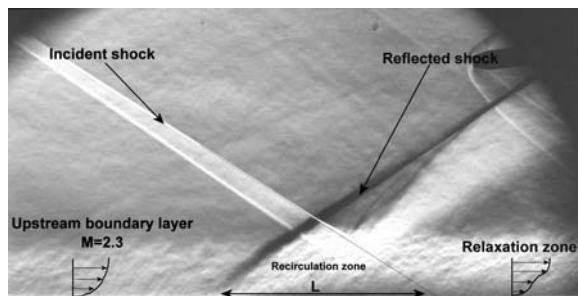


Figure 5 : shock wave/boundary layer interaction observation at IUSTI wind tunnel

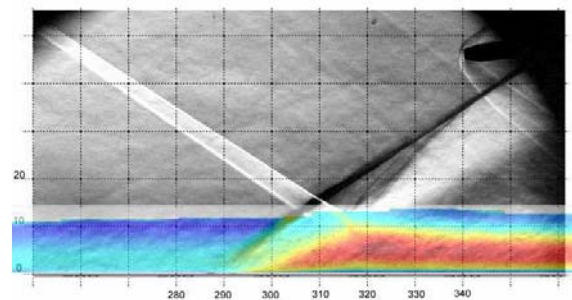


Figure 6 : speed fluctuations obtained through PIV measurements

The physical understanding aspect has been addressed through the construction of a simple model linking the low frequency unsteadiness of the shock to the breath of the recirculation bubble [3]. A major conclusion of this study is that this shock unsteadiness is mainly driven by the downstream flow.

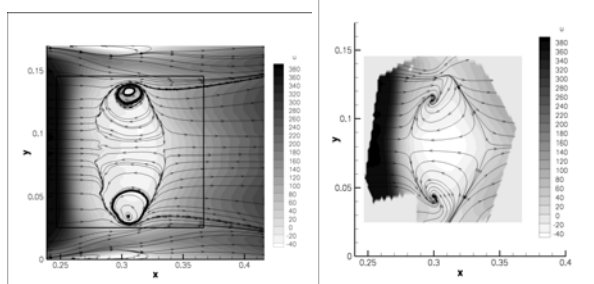


Figure 7 : Longitudinal velocity at 1.2 mm from the wall. Left: SDES; Right: PIV.

The analysis of the results obtained during this campaign goes on, and some improvements are under consideration to reduce the influence of the walls, or increase the representativeness of the tests via an axisymmetric set-up.

In addition to these studies, an activity is on progress at SINUMEF in order to numerically reproduce the shock unsteadiness in this interaction through the solving of the stability equations for incompressible and compressible (subsonic and supersonic) flows [5].

2.2 FSS and RSS

FSS nozzles

The Free Shock Separation has been investigated thanks to Truncated Ideal Nozzles at ONERA and LEA [6]. For this latest experiment, three TIC nozzles, having the same profile inspired from DLR studies but with different scales (1:1.5; 1:1 and 1:0.75) have been tested to study the level and frequency similitude of side-loads. It has been observed that the evolution of side-loads versus NPR was nearly the same for the two smallest nozzles (1:1 and 1:0.75) with a maximum of side loads at NPR=25. As expected, at the same NPR, the side-loads on the 1:0.75 scaled nozzle are smaller than those of the 1:1 scaled nozzle. Preliminary conclusion is that there is a weak influence of the Reynolds number, which should not be contradicted for this nozzle side load phenomenon, which is governed by the shock wave – boundary layer interaction and characterized by a fully developed turbulence.

This LEA experiment was then used numerically by ONERA [7], LEA and CORIA, to investigate the importance of the turbulence model for the prediction of the separation location, and also to understand the physical phenomena at stake for the side loads in steady conditions.

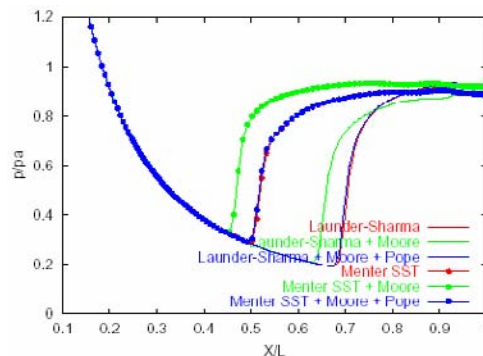
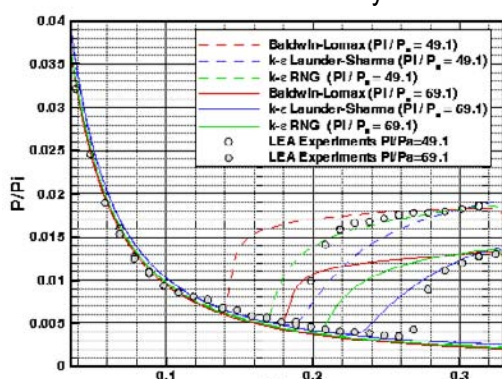


Figure 8 : separation location prediction by ONERA (left) and LEA (right) numerical tools

The Launder Sharma model shows a good agreement with the experimental results (Figure 8), and the study concluded to the strong influence of the turbulence model for the prediction of the separation (location, pressure

levels). Moreover, URANS computations [7] gave a good agreement with the experiment for the side loads evaluation, and showed that the pressure pulsations in the turbulent shear layer behind the separation had a great influence on the side loads level.

Furthermore, the statistical analysis of these unsteady computational results has shown that the side load modulus was distributed according to a chi-2 probability law, without any privileged azimuth, which is not unexpected from a numerical simulation performed with axisymmetric limit conditions.

From these studies, it can be concluded that, in Free Shock Separation, the aerodynamic causes of side loads are 1) the shock oscillations associated with high levels of pressure fluctuations in the shock-wave / boundary-layer interaction region, and 2) the self-sustained pressure fluctuations in the recirculating fluid region, which levels are lower but which exert on the whole separated wall. These two antagonist contributions on the side loads are well illustrated by the Onera side load semi-empirical model which is based on a pressure rms model[8].

RSS nozzles

The Restricted Shock Separation has been investigated experimentally in TOC nozzles at ONERA and LEA ([12],[13]). The ONERA set-up was designed to understand the influence of the film cooling, and the LEA one was specially equipped for the side loads measurements. TOC nozzles present both FSS and RSS configurations, depending on the NPR. A particularity of the FSS in this kind of nozzle is the cap-shock pattern occurring when the internal shock intersects the Mach disk.

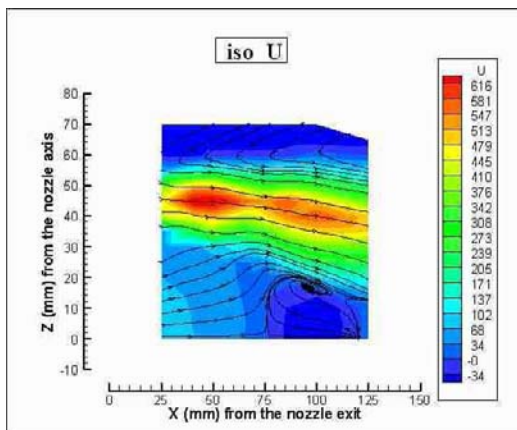


Figure 9 :- Recirculating bubble (LDV measurements in the TOC nozzle tested at Onera)

An outstanding fact of this cap-shock pattern is the existence of a recirculation bubble downstream the normal shock. It was first pointed out by several RANS computations [9], and then evidenced by a qualitative characterization of a negative streamwise velocity zone in DLRP6.2 bench thanks to threads fixed on wires located in the jet of the overexpanded DLRTOC nozzle [9]. A first quantitative measurement of this particular nozzle flow with cap-shock structure and recirculating bubble inside the jet has also been made in the ONERA R2Ch wind tunnel with Laser Velocimetry probings [11].

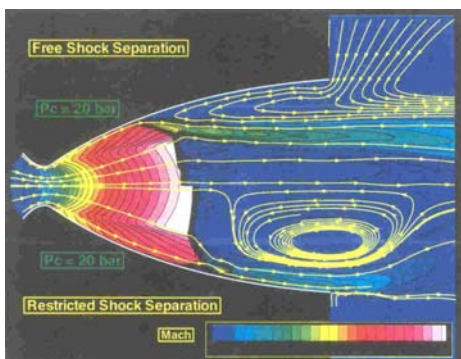


Figure 10 : Computed FSS and RSS flow regimes in the LEATOC nozzle at NPR=20

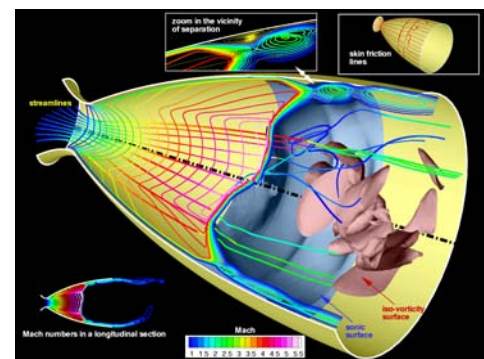


Figure 11 : LEATOC nozzle jet structure in RSS regime (DES-FLU3M calculation)

Both RSS and FSS regimes have been evidenced numerically in the LEATOC nozzle by RANS simulations (see Figure 10 and [14] for the conclusions by ONERA), and showed an hysteresis effect depending on the increasing or decreasing nature of the NPR.

A first computation of the RSS regime with a DES model can be found in [14] (see also Figure 11). Most recently, a DES simulation of the end-effect in this very nozzle has been undertaken by ONERA [16]. The end-effect regime is the period in the RSS regime when the reattachment line reaches the nozzle lip, allowing the recirculation bubble to open to the ambient atmosphere. This particular time of the flow is characterized by large pressure fluctuations which were well reproduced by the DES simulations.

2.3 Transient effects

FSS-RSS transitions

During start-up or shut-down in an overexpanded TOC nozzle, the side-load peaks appear when a transition (FSS-RSS, or RSS-FSS) occurs. This has been illustrated during the side load testing of a TOC nozzle at LEA/Poitiers

(Figure 12) which showed three peaks of the rms side effort versus NPR. Let us note that LEA tests were running at stabilized NPR conditions.

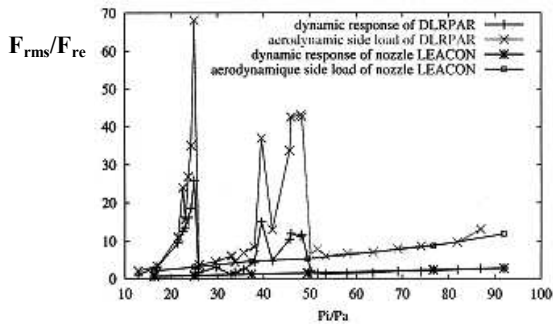


Figure 12 : Rms side-load regimes in the TOC nozzle tested at LEA

The causes of the FSS-RSS transition are not well elucidated. Indeed, the cap-shock pattern can co-exist with the FSS regime, and the transition to the RSS pattern is not systematic in all nozzles with internal shock. Some of the suspected parameters are the proximity of the internal shock relatively to the wall, the nozzle area-ratio and the pressure fluctuation levels in the initially free-separated region delimited by the wall and the separated dissipative layer. ONERA and CORIA, [14], [15], have numerically studied the transition in LEATOC nozzle, and have reproduced the hysteresis and the FSS-RSS transition observed experimentally.

Influence of the film cooling

Due to the high temperature environment in the nozzle flow, some structures use a film cooling to master the wall heat fluxes. This film cooling, and the pressure ramping of its injection, have a strong influence on the shock and separation structures of the flow which have to be assessed. Therefore, a thorough experimental analysis of this influence has been achieved [17], using the cold gas R2Ch wind tunnel of ONERA, with a subscale nozzle equipped by a wall film injection (see Figure 13 and Figure 14).

The main nozzle and wall film injection were separately fed, and bulkheads and jet spreading devices were implemented in order to control and homogenize the stagnation pressure inside each cavity of the film injection chamber.

The transient effect of the main jet on a steady wall injection showed greater side loads levels than the transient effect of the wall injection on a steady main flow. Indeed, when the jet is stabilized, the increasing mass flow rate of the film has a great influence on the shock position, but due to its rather axisymmetric nature, the side loads activity is rather low. An asymmetric wall transient injection on a steady jet has been tested as well.



Figure 13 : Experimental set-up with wall film cooling in the R2Ch wind tunnel

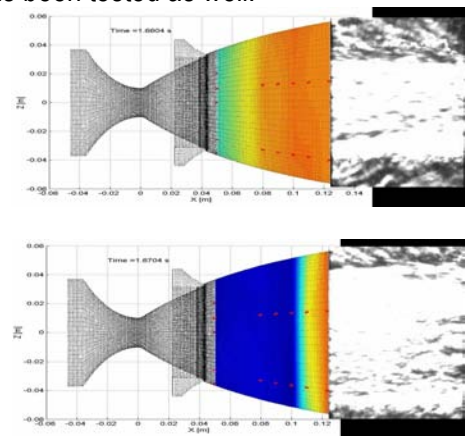


Figure 14 : Influence of the wall film injection on the nozzle flow for a critical NPR

Pressure ramping effect

The dynamic behaviour of the nozzle structure in transient conditions, and more precisely the characterisation of the side loads, is under great consideration for a better evaluation of the loads endured by the structure during this specific phase of the engine life.

An experimental set-up has been developed at R2Ch ONERA wind tunnel to answer this need (see Figure 15). The bench was equipped by a specific unsteady balance composed of 3 Kistler® force sensors, and by a pressure reducer in order to control the generating pressure rise to a maximum of 3ms for achieving similarity. An auxiliary jet

pipe discharging a supersonic jet near the main jet was also implemented so as to simulate the influence of a turbopump exhaust gas line (Figure 16).

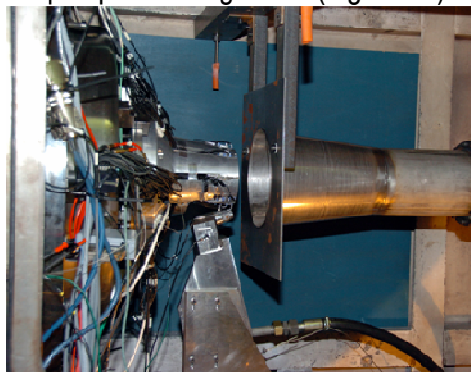


Figure 15: Assembly in R2Ch test section

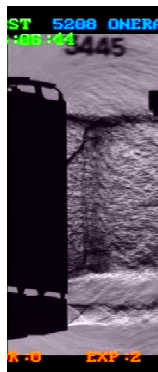


Figure 16: Schlieren photography

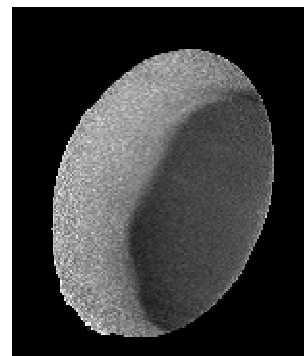


Figure 17: Unsteady PSP image of the shock foot in the nozzle

Therefore, this set-up was able to reproduce a chamber pressure rise, and to measure the unsteady dynamic response of the structure. To better analyze the flow structures, the model was equipped with 60 static pressure taps, 4 accelerometers and 66 non-steady pressure taps, and high-speed visualisation of Schlieren photography images (8000i/s) were performed by a digital camera (Figure 16). Moreover, a model dedicated to the unsteady pressure-sensitive paint (uPSP) measurement with a short response time (less than 200 μ s), allowed for the implementation of this technique and the visualisation of the buffeting of the shock (see Figure 17), even during the stabilised phase of the flow.

3. FLUID/STRUCTURE INTERACTION

3.1 Numerical work on the Pekkari model

The elastic behaviour of the nozzle structure for rocket engines is addressed through the use of the Pekkari model [18], which relies on a simplified stability analysis; the movement of a recompression shock along the wall of a flexible nozzle is simply modeled by a piston analogy, and the shifting of the aeroelastic frequencies due to this movement is then deduced from this modeling (eigenvalue analysis).

An extended version of this model has been developed by CORIA and CNES in the ATAC program [19], and is able to capture some specific elastic behaviour of the nozzle (flutter), with a mass/spring analogy.

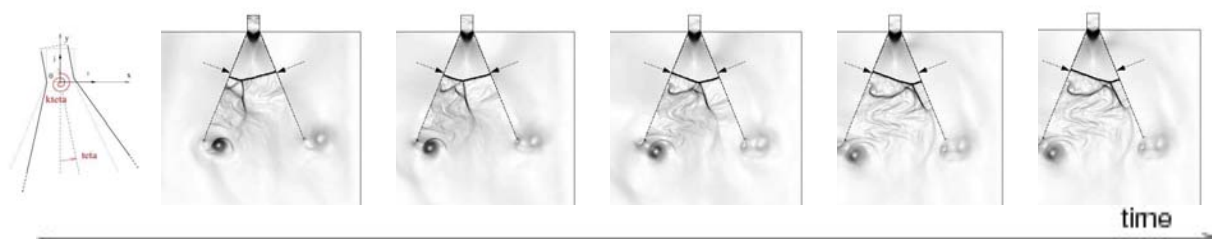


Figure 18: Transversal wave resulting from coupling at a critical frequency (fluid/structure simulations)

The ongoing activities at UTC [20] are dealing with the influence of rigid body motions (rotation around the cardan axis) on the aeroelastic response of the structure. Indeed, the very hypothesis of the Pekkari modele (piston approximation) can not take into account such an influence, and especially the modification of the flow structure (see Figure 18). A modification of the algebric formulation of the model is under investigation to better integrate this kind of phenomenon.

3.2 Test campaign on a flexible nozzle



Figure 19: flexible nozzle at LEA

An epoxy flexible TIC nozzle has been experimentally tested at LEA in 2001 under ONERA supervision (see Figure 19 and [21]). The tests showed the dynamic response of the structure (1st flexion mode) for low NPR. The unstable ovalisation mode foreseen by the Pekkari model at higher NPR (54) was also reproduced but lead to the destruction of the nozzle since its displacements could not be absorbed by the safety system.

A new experimental set-up is under investigation in order to achieve the objectives of the first campaigns relative to the Pekkari model. This test, equipped with the appropriate pressure sensors, would also be a valuable case for the validation of coupled fluid/structure numerical tools.

4. THERMAL LOADS

In liquid-rocket nozzles, the high level of stagnation enthalpy induces high heat fluxes on the wall of the nozzle extension. As already mentioned in § 2, some nozzle structures use a film cooling to master these wall heat fluxes. Unfortunately, in this case, the flow separation occurring at the end of the nozzle is an aggravating factor for two reasons: **1/** the film cooling can not operate properly in case of a flow separation; **2/** a combustion can occur between the film cooling gas (usually H_2) and the air oxygen coming from the separated region. From a general point of view, the physical mechanisms leading to these fluxes need to be assessed either experimentally or numerically, in order to better dimension the thermal behaviour of the nozzle extension.

4.1 Hot gas test campaign at Mascotte (ONERA bench)

An experimental set-up has been implemented in the Mascotte test bench in order to observe the reactive flow of a planar nozzle fed with hot gases resulting from a liquid oxygen/gaseous hydrogen (LOX/H_2) combustion (see nozzle mounting in Figure 20). The choice of the planar configuration was made in order to better visualize and measure the flow structure. This device can reach stagnation temperature of nearly 2500K in the combustion chamber and can reproduce a gaseous hydrogen film-cooling at the nozzle wall.

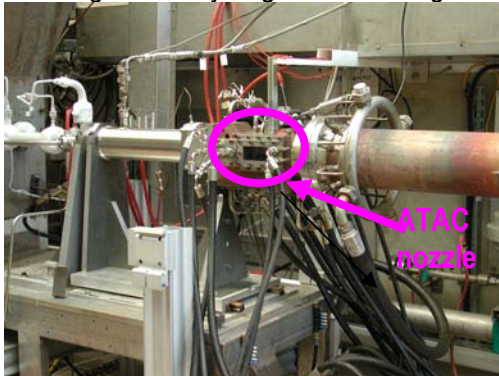


Figure 20 : ATAC nozzle at Mascotte

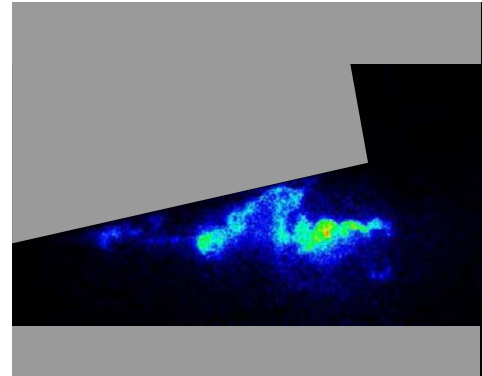


Figure 21 : PLIF-OH measurements on the ATAC nozzle

The tests were operated for three stagnation pressures (20, 40 or 60 b) related to three separation regimes (fully separated, nearly separated, fully adapted), and for two mixing ratios (1.7 or 2.7), with or without film cooling injection (H_2 or He). The set-up was equipped with steady and unsteady pressure transducers, in addition to fluxmeters. Moreover, PLIF-OH emission measurements took place in order to visualize the possible combustion zones (identified by an increased concentration of OH). These measurements did show the presence of a combustion area in the separated mixing layer and in the re-circulation region of the overexpanded nozzle (see Figure 21).

This test campaign was a success since it led to the observation of combustion areas in the separated region, for different chamber pressures and mixing ratios. However, without velocimetry measurements, these tests can not be fully used for the validation of numerical tools, and some assumptions still remain to be made for the proper simulation of this reactive flow. A PIV campaign is foreseen as soon as the bench is available.

4.2 New experimental set up on progress at Mascotte

An adaptation of the Mascotte bench is currently on-going in order to run tests with higher mixing ratios, for a better representativity of the thermal conditions in rocket engines. Moreover, the test campaigns foresee an intense use of optical measurement techniques such as OH-PLIF, PIV or DRASC, with a statistical approach, and therefore need long duration runs. The dual need for high mixing ratios and long duration runs implies strong thermal constraint on the set-up. A special care has thus been taken on the dimensioning of the cooling of the different parts of the structure. This set-up has also been widely equipped in fluxmeters in order to build a data base for the validation of numerical tools.

The manufacturing of this new set-up is currently on finalisation and the first test campaigns are foreseen by October 2009.

4.3 Numerical simulations

Some numerical simulations have been performed by ONERA and LMEE with the data available from the ATAC campaign at Mascotte.

The activity at ONERA was performed with Cedre, for the fully separated case ($P=20b$) [22]. The first simulations used two kinds of RANS turbulence model: $k-\omega$ SST and $k-l$. Neither of them was able to reproduce the presence of a combustion area inside the nozzle, in the separated region.

A LES approach for such a geometry, even if more realistic, can not be foreseen due the prohibitive mesh and CPU costs. Furthermore, the DDES model used in the frame of the ONERA side loads studies [22] gives very good results, with CPU costs much more mastered. Therefore, this kind of modelisation was implemented in Cedre, but based on the $k-\omega$ SST model instead of the Spalart Allmaras one for the RANS part. As a first step, 2D computations were done even if the 2D approach can not be approved due to the 3D nature of the geometry, and of the DDES formulation. They showed already a good agreement with the experiment (see Figure 22 and Figure 23), since the combustion area inside the nozzle in the separation region could be reproduced. 3D simulations are currently on-going and will show the influence of these three-dimensional effects on the numerical behaviour of the flow.

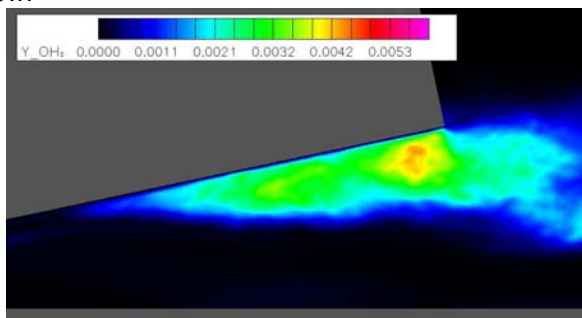


Figure 22 : average field of YOH evidenced by PLIF

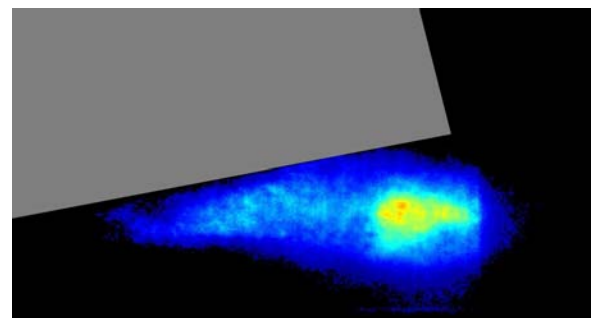


Figure 23 : average field of YOH evidenced by DDES

These test cases are also simulated by LMEE with the Fastran code, and should be computed this year by IUSTI with Marcus. For both these activities, the turbulence is computed through RANS models, but a sensitivity analysis is foreseen with regard to the combustion modelisation (based on Eklund formulation Cedre).

Some numerical developments are on progress at CORIA to take into account the reactive nature of the flow, focusing on the compressible mixing layer as a first step with DNS simulations. The thermal transfers should then be investigated, which requires the development of a DES turbulence model in the numerical tool, since DNS simulations can not be foreseen at such a scale.

5. CONCLUSION

This paper presents a brief survey of the research works on Nozzle Aerodynamics for Launchers undertaken within the CNES-ONERA ATAC program.

The side loads phenomenon has first been addressed in steady conditions. To start with, the shock wave/ boundary layer interaction has been studied experimentally and lead to the construction of a simple model for the prediction of the shock unsteadiness frequency. This experimental case has also been used for the validation of numerical tool in LES but also with innovative modelisations of the turbulence.

Moreover, many test campaigns have investigated the different shock structures (RSS or FSS) occurring in an overexpanded nozzle. The results were used by numerical tool to characterize the turbulence model the best suited for the prediction of the separation location. They also permitted the elaboration of a semi-empirical model for the prediction of side loads. Both experimental and numerical studies were used to better understand the driving factors of side loads in steady conditions, and highlighted the importance of the recirculation bubble in the cap-shock pattern.

The side loads in unsteady conditions have mainly been addressed experimentally since the time scale of this phenomenon in transient regime has great consequences on the high CPU cost. However, considering the breakthrough of DES simulations, it is currently under consideration. Up to now, the experimental studies have investigated the FSS-RSS transition, the film cooling effects and the start up (with a chamber pressure rise) effects. Furthermore, the aeroelastic behaviour of the nozzle is being studied numerically through the use of the Pekkari model, which has seen many improvements within the ATAC program, for a better representativity. A test campaign showed a good agreement with the prediction issued from the Pekkari model.

The thermal loads were first investigated in an experimental test campaign at moderate mixture ratio, and showed a recombustion of the flow in the separated area inside the nozzle. A new set-up for higher mixture ratios is currently

manufactured and is expected to give precious information on the thermal transfers at walls. Indeed, this test case is foreseen for the validation of the numerical tools, which already showed good agreement with the first experimental test campaign.

ACKNOWLEDGEMENTS

Special thanks are addressed to the industrials SNECMA Moteurs and ASTRIUM-ST, and the French research laboratories of CNRS (LMEE, LEA, CORIA, IUSTI, UTC, ENSAM), which contribute to the ATAC scientific project. The ATAC group are grateful for the fruitful scientific exchanges with their European colleagues of the FSCD framework, in particular EADS-Astrium, Volvo Aero, DLR and FOI.

REFERENCES

- [1] FREY, M. & HAGEMANN G. (2000). Restricted Shock Separation in Rocket Nozzles. *AIAA Journal of Propulsion and Power*, vol.16, No.3, pp 478-484.
- [2] DUPONT, P., HADDAD, C., ARDISOINE, J. & DEBIEVE, J. (2005). Space and time organisation of a shock wave/turbulent boundary layer interaction. *Aerospace Science and Technology*, Vol. 9, Issue 7, 561-572. 7, 10.
- [3] PIPONNIAU, S., DUSSAUGE, J.P., DEBIEVE, J.F. & DUPONT, P. (2009). A simple model for low-frequency unsteadiness in shock-induced separation. *Journal of Fluid Mechanics*, Vol. 629 , 87 – 108.
- [4] GARNIER, E. Stimulated Detached Eddy Simulation of three-dimensional shock/boundary layer interaction. *Shock Waves*, to be issued.
- [5] MERLE, X. & ROBINET, J.C. (2008). Stability Analysis of Shock Waves/Boundary Layers Interaction. *18th International Shock Interaction Symposium*.
- [6] GIRARD, S. (1999). Etude des charges latérales dans une tuyère supersonique détendue. *Thèse de doctorat de l'université de Poitiers*.
- [7] DECK, S., GUILLEN, P. (2002). Numerical Simulation of Side Loads in an Ideal Truncated Nozzle. *Journal of Propulsion and Power*, Vol. 18, No 2.
- [8] REIJASSE, P. (2005). Aérodynamique des tuyères propulsives en sur-détente: décollement libre et charges latérales en régime stabilisé (Aerodynamics of overexpanded propulsive nozzles : free separation and side loads in stabilized regime). *Ph.D. thesis, University of Paris 6 – Jussieu*.
- [9] FREY M. , RYDÉN R., ALZIARY DE ROQUEFORT T., HAGEMANN G., JAMES P., KACHLER T., REIJASSE P., SCHWANE R. & STARK R.(2002). European cooperation on flow separation control. *4th International Conference on Launcher Technology "Space Launcher Liquid Propulsion", Liège, Belgium*.
- [10] ONOFRI, M., & NASUTI, F.(1999): The physical origins of side loads in rocket nozzles AIAA 99-2587
- [11] REIJASSE P., BOUVIER F. & SERVEL P. (2002). Experimental and numerical investigation of the cap-shock structure in overexpanded thrust-optimized nozzles. *West-East High Speed Flow Field Conference*.
- [12] NGUYEN, A.T. (2005). Décollement instationnaire et charges latérales dans les tuyères propulsives. *PhD thesis, Université de Poitiers, Dpt Sciences de l'ingénieur, Poitiers*.
- [13] NGUYEN, A.T., DENIAU, H. , GIRARD, S. & ALZIARY DE ROQUEFORT, T. (2003). Unsteadiness of Flow Separation and End-Effects Regime in a Thrust-Optimized Contour Rocket Nozzle. *Int. J. Flow Turbulence and Combustion*, Vol 71, No. 1, pp161-181.
- [14] DECK S. & NGUYEN A.T. (2004). Unsteady Side Loads in a Thrust Optimized ContourNozzle at Hysteresis regime. *AIAA Journal*, vol.42, No.9, pp 1878-1888.

- [15] NEBBACHE, A. & PILINSKI, C. (2006). Pulsatory phenomenon in a thrust-optimized contour nozzle. *Aerospace Science and Technology*, Vol. 10, No. 4, pp 295-308,2006.
- [16] DECK, S. (2009). Delayed Detached Eddy Simulation of the end-effect regime and side-loads in an overexpanded nozzle flow. *Shock Waves*.
- [17] REIJASSE, P. & BOCCALETTO, L. (2008). Influence of film cooling on nozzle side loads. *46th AIAA Aerospace Sciences. AIAA 2008-392*.
- [18] PEKKARI, L. O. (1993). Aeroelastic Stability of Supersonic Nozzles with Separated Flow. *AIAA, 29th Joint Propulsion - Conference and Exhibit, Monterey, CA*.
- [19] LEFRANCOIS, E., DHATT, G. & VANDROMME, D. (2000). Numerical Study of the Aeroelastic Stability of an Overexpanded Rocket Nozzle. *Revue européenne des elements finis*, Vol. 9, N° 6/2000, p 727-762.
- [20] LEFRANCOIS, E. (2008). Side-loads and rigid body motions application to a 2D overexpanded nozzle engine.. *18th International Shock Interaction Symposium*.
- [21] MOREAUX, N., GIRARD, S. (2003). Experimental Assessment of aeroelastic coupling in a rocket engine nozzle. *IFASD*
- [22] SAINTE-ROSE, B. , BERTIER, N. , DECK, S. & DUPOIRIEUX.,F. (2008). Numerical Simulation of a Reactive Flow in an Overexpanded Nozzle. *6th ESA Aerothermodynamics of Space Vehicles*.